Fabrication and characterization of an agarose and GelMA hybrid scaffold for adipose tissue regeneration

Ana Margarida Teixeira[1,2,3], Lana Van Damme[3], Sandra Van Vlierberghe[3] and Pedro Martins[2,4] *

[1]Faculty of Engineering of University of Porto, Porto, Portugal
[2] Associated Laboratory of Energy, Transports and Aeronautics (LAETA), Institute of Science and Innovation in Mechanical and Industrial Engineering (INEGI), Porto, Portugal
[3]Polymer Chemistry and Biomaterials Group, Centre of Macromolecular Chemistry (CMaC), Department of Organic and Macromolecular Chemistry, Ghent University, Ghent, Belgium
[4] Aragonese Foundation for Research and Development (ARAID), Instituto de Investigación en Ingeniería de Aragón (i3A), Universidad de Zaragoza, Zaragoza, Spain

Abstract

Purpose - To overcome the drawbacks of current clinical practices in breast reconstruction, tissue engineering is currently the most promising field to create improved alternatives and new strategies. Biomaterials that mimic the physico-chemical and biological properties of the native extracellular matrix (ECM), e.g. hydrogels, have been characterized and seeded with cells, with the purpose of promoting the regeneration of tissues. In this study, a new hydrogel blend was produced and characterized for adipose tissue regeneration purposes.
Design/Methodology/Approach - Blends of agarose and gelatin-methacryloyl (GelMA) were produced in different weight percentage ratios (100:0, 75:25 and 50:50 of agarose:GelMA). Indirect 3D printed scaffolds and 2D discs were fabricated and characterized in terms of physico-chemical and biological properties in the presence of adipose tissue-derived stem cells (ADSCs).
Findings - Both scaffolds and discs presented a good gel fraction (>90% for most of the samples) and a swelling degree >17% for all samples. In terms of stiffness, the results varied from 2.86kPa to 25.11kPa depending on the testing conditions (i.e. testing temperature) and sample chemical composition. Rheology analysis showed that the storage modulus was higher than the loss modulus, indicating a more elastic behavior. Moreover, the scaffolds with GelMA could support cell adhesion and proliferation, with a viability higher than the control (i.e. tissue culture plastic, TCP) by day 14 (118% and 128% for the ratios 75:25 and 50:50, respectively), showing that 50:50 is the optimum ratio composition.
Originality/Value - The blend of agarose and GelMA presented in this study offers a new and promising approach towards adipose tissue regeneration.

Keywords— Indirect 3D printing, Agarose, Gelatin-methacryloyl, Scaffolds, Adipose tissue-derived stem cells

I. Introduction

Tissue engineering is an appealing field to provide alternatives to current prostheses and implants. To replace damaged tissues or organs, the ideal solution would provide cell carriers with similar mechanical properties as the targeted tissue. For instance, in breast reconstruction, tissue engineering can overcome the drawbacks associated with breast silicone implants or autologous tissue, which are currently the clinical procedures performed (Teixeira & Martins 2023, Bülow et al. 2023, Peirsman et al. 2023).

Therefore, studies have been carried out in order to develop biomaterials able to regenerate breast tissue, mainly composed by adipose, glandular and fibrous tissues

To regenerate a specific tissue, the biomaterial used has a fundamental role since its mechanical

*Corresponding author: pmartins@unizar.es

and chemical properties will affect cell adhesion, proliferation and differentiation (O'Halloran et al. 2018, Aliabouzar et al. 2018, Cleversey et al. 2019, Donnely et al. 2020, Zhou et al. 2020). In the case of adipose tissue regeneration, natural polymers such as hydrogels (e.g. gelatine, alginate (Bülow et al. 2023)) have been widely investigated due to their biocompatibility, low inflammation and suitable mechanical properties, mimicking accurately the natural extracellular matrix (ECM) (O'Halloran et al. 2018, Zigon-Branc et al. 2019, Bramhe et al. 2024). In literature, hydrogels derived from gelatin have been widely studied for this purpose (Ovsianikov et al. 2010, Van Hoorick et al. 2015, Markovic et al. 2015, Tytgat et al. 2019, Van Damme et al. 2020). Their physical properties mimic adipose tissue, being able to promote cell adhesion, proliferation and differentiation.

Even though agarose is not commonly reported as a solution for adipose tissue regeneration, a previous study showed that an agarose phantom also mimics the mechanical properties of adipose breast tissue (Teixeira & Martins 2020). Agarose is a natural linear polysaccharide that presents tunable mechanical properties, self-gelling properties, controllable permeation to oxygen and nutrients, mimics the physical properties of ECM, is biocompatible, is electrically neutral and exhibits swelling behavior (Dravid et al. 2022, Zarrintaj et al. 2018, Jiang et al. 2023). However, it is a biomaterial that exhibits poor cell interaction since it does not have native ligands for cells to attach (Awad et al. 2004, Imani et al. 2012). Therefore, it is an inert material, which is a major drawback when using it for the regeneration of a tissue. To overcome this disadvantage, some authors have added gelatin, since it is a natural hydrogel with cell-interactive properties (i.e. it contains tripeptide Arginine-Glycine-Aspartic acid (RGD) sequences in its structure, which interacts with cell surface integrins (Van Hoorick et al. 2015)) (Dravid et al. 2022, Imani et al. 2012). Dravid et al. (2022) focused on extrusion-based printing and developed an agarose-gelatin bioink, testing and characterizing different polymer concentrations. All the bioinks showed rheological, mechanical and swelling properties suitable for 3D printing and cell encapsulation, exhibiting shear-thinning and pseudo-plastic behavior. Using SH-SY5Y cells, which differentiated into neuronal-like cells, the cell viability was higher than 90% for all bioinks. In addition, by combining agarose with gelatin at different weight percentage ratios, Imani et al. (2012) proposed a cell encapsulation approach for cryopreserved hamster ovary cells. The ratios of 75:25 and 50:50 of agarose to gelatin showed the best gel point, near body temperature, and formed microcapsules with high encapsulation resistance (more than 90% of the microcapsules remained intact). Cell viability was for most of the ratios higher than 90%, being the maximum result for the ratio 50:50, followed by the ratio 75:25. In terms of cell adhesion and growth, it was observed that these decreased upon increasing the agarose concentration since cells tended to aggregate more on the hydrogel surface.

Using adipose tissue-derived stem cells (ADSCs), commonly used for adipose tissue regeneration (Peirsman et al. 2023), Awad et al. (2004) compared their chondrogenic differentiation using agarose, alginate and gelatin scaffolds. In the agarose and alginate scaffolds, the cells exhibited a spherical morphology, while for the gelatin scaffold, the cells had a fibroblast-like morphology. In chondrogenic conditions, agarose scaffolds presented significantly lower biosynthesis rates of proteins and proteoglycans, as quantified by [3H]-proline and [35S]-sulfate incorporation, respectively. Also, in chondrogenic conditions, the DNA and hydroxyproline contents were higher for the gelatin scaffolds on days 14 and 28, while there was no significant difference between scaffolds for sulfated glycosaminoglycans. In terms of mechanical properties, all scaffolds showed a viscoelastic

behavior, with the equilibrium shear modulus and complex shear modulus increasing over time for all scaffolds, being significantly associated to the increase in sulfated glycosaminoglycans content. The equilibrium compressive modulus decreased between days 0 and 14 for the agarose and alginate scaffolds, and increased over time for the gelatin scaffolds, being related to the hydroxyproline content.

Gelatin is an interesting hydrogel since it is bioresorbable (Bulcke et al. 2000), biocompatible and has low cost (Dravid et al. 2022, Xu et al. 2022). However, when used alone, due to the low melting point (Bulcke et al. 2000), gelatin forms weak structures (Imani et al. 2012) which lack mechanical robustness (Dravid et al. 2022, Li et al. 2023), being unstable and dissolved at physiological conditions (i.e. 37ºC) which is a limitation for final applications (Van Hoorick et al. 2015, Xu et al. 2022, Bramhe et al. 2024). To produce chemically stable structures, methacrylation (i.e. gelatin-methacryloyl, GelMA) is a strategy to overcome the main drawback of gelatin, since the melting point of GelMA is higher (Bulcke et al. 2000), allowing the development of stable structures at body temperature while maintaining the biomimetic properties of gelatin.

Moreover, the design of hybrid biomaterials is also a strategy, by combining hydrogels to highlight the positive features and overcome the negative ones, achieving an improved solution. Therefore, in this study, we combined GelMA with agarose and studied its potential for tissue engineering.

To the best of our knowledge, to date, there is no information available in literature regarding agarose-GelMA scaffolds seeded with ADSCs to serve adipose tissue regeneration. Therefore, the aim of this work was to develop and characterize structures constituting agarose-GelMA blends, using different weight percentage ratios, to serve adipose tissue regeneration.

II. Materials and Methods

i. Materials

For this study, gelatin type B (isolated from bovine skin) was supplied by Rousselot (Ghent, Belgium). Agarose was purchased from MP Biomedicals (QA- Agarose Multipurpose, AGAP0100). Chloroform was acquired from Chem-Lab NV (Zedelgem, Belgium). Dulbecco's Phosphate Buffered Saline (PBS), Dulbecco's modified Eagle's medium (DMEM), fetal bovine serum (FBS), penicillin/streptomycin, Trypsin and Trypan blue were purchased from Gibco (Life Technologies, California). ADSCs (SCC038), calcein-acetoxymethyl (Ca-AM), propidium iodide (PI), methacrylic anhydride, D_2O and Spectrapor dialysis membranes (MWCO 12,000-14,000 Da) were obtained from Merck Life Science BV (Hoeilaart, Belgium). For the cell counting, a Burker's chamber (Marienfeld Superior, Thermo Fisher Scientific Inc.) was used.

ii. Sample Preparation

ii.1. Development of Gelatin-Methacryloyl

GelMA was developed via reaction of gelatin with methacrylic anhydride, following the protocol of Bulcke et al. (2000). Briefly, following dissolution of 100 g (38.5 mmol amines) of gelatin in 1 L of phosphate buffer (pH 7.8) at 40ºC, 14.34 mL methacrylic anhydride (96.25 mmol) was added under vigorous stirring. After 1 hour of reaction, dialysis against distilled water was performed for 24h at 40ºC, in order to remove the unreacted methacrylic anhydride and the formed methacrylic acid (a side product of the reaction). The GelMA obtained was then frozen at -20ºC and freeze-dried. The degree of substitution, defined as the percentage of amino groups that were modified, was measured using ^{1}H-NMR spectroscopy at 40ºC in D_2O in a Bruker WH 500 MHz NMR

spectrometer.

ii.2. Blend Solution Preparation

A solution of 3% w/v agarose (quantity empirically chosen to guarantee scaffolds printability) with 10% w/v GelMA (being the best compromise between scaffold integrity and cell viability (Van Hoorick et al. 2015)) was prepared in different ratios (100:0, 75:25 and 50:50 (v/v) of agarose to GelMA) at a final volume of 50 mL. Firstly, the agarose was dissolved in double-distilled water (ddH_2O) at 90ºC and GelMA was dissolved in ddH_2O at 40ºC in a separate flask. The photoinitiator Li-TPO-L at 4% mol (with respect to the methacrylamide moieties) was added to the GelMA solution and the mixture was mixed until homogeneous. The GelMA with the photoinitiator blend was finally added to the agarose at 50ºC. The photoinitiator LAP was synthesized following the protocol of Tromayer et al. (2018).

ii.3. 2D Discs Fabrication

For the discs, the solution was poured between two glass plates with a mold of 1 mm height in the middle composed by circles of 14 mm diameter. The discs were first placed in the fridge for physical gelation and then, they were photocrosslinked for 30 minutes under UV-A irradiation (365 nm, 9.5 mW/cm^2). These samples were characterized in terms of mass swelling ratio, gel fraction and rheology.

ii.4. 3D Scaffolds Fabrication

Polylactic acid (PLA) molds, with dimensions of 10x10x10 mm^3, pore size of 1x1 mm^2 and linewidth of 1 mm, were produced using a Ultimaker 3 printer (Ultimaker, Gerldermalsen, the Netherlands), via fused filament fabrication (FFF). The CAD design corresponded to the negative mold of the scaffold and was printed via the Cura 13.06.4 software with a speed of 60 mm/s at 210 ºC.

To facilitate the injection of material into the mold, a surface treatment was applied to increase the hydrophilicity of the PLA. For most of the scaffolds, low-pressure plasma treatment (Diener electronic, Germany) was applied using oxygen during 2.5 minutes at 0.8 bar. However, prior to mechanical testing, alkali treatment was applied instead. According to Donate et al. (2021), the water contact angle was similar to the one observed for a PLA surface subjected to oxygen plasma treatment and NaOH treatment. In this way, for the mechanical characterization, the molds of PLA were immersed in a solution of 1 N NaOH for 1h at room temperature, then they were rinsed with purified water, washed with 0.1 N HCl solution and rinsed again with purified water.

After the surface treatment, the molds were submerged in the final solution of agarose and GelMA and the flask was covered with aluminum foil. Vacuum was performed a minimum of 3 times with 30 minutes interval between each time point, to ensure sufficient penetration inside the molds and removal of any air bubbles. Then, the scaffolds were photocrosslinked under UV-A irradiation for 1h and then, placed in the fridge for 20 minutes to ensure solidification of the agarose. Afterwards, the scaffolds were put in a flask with chloroform for PLA dissolution during 48h, with constant stirring. The chloroform was changed twice a day.

The scaffolds produced were subjected to physico-chemical characterization (i.e. mass swelling ratio, gel fraction and compression tests) and to biological characterization (i.e. MTS assay and live/dead assay).

iii. Physico-Chemical Characterization

iii.1. Mass Swelling Ratio

After incubating for 24h at 37 ºC in ddH_2O, the swollen samples were weighed in the equilib-

rium state (W_s). Then the samples were frozen overnight, followed by lyophilization for 24h. The dry sample was then weighted again (W_d). Using these two measures of mass, the mass swelling ratio was calculated using the following equation:

$$Mass\ Swelling\ Ratio = \frac{W_s}{W_d} \quad (1)$$

where W_s is the swollen mass and W_d is the dry mass.

This characterization was performed on 3D scaffolds and 2D discs, using a minimum of 3 samples for each test

iii.2. Gel Fraction

First, the samples were placed in the freezer for 24h, lyophilized afterwards and the dry mass was obtained (W_0). Next, the samples were put in ddH_2O at 37 ºC for 24h for equilibrium swelling and were then lyophilized again for 24h. The new dry mass was obtained (W_{de}) and the gel fraction was calculated using the following equation:

$$Gel\ Fraction\ (\%) = \frac{W_{de}}{W_0} \times 100 \quad (2)$$

where W_0 is the initial dry mass and W_{de} is the dry mass after sample swelling.

This characterization was performed on 3D scaffolds and 2D discs, using a minimum of 3 samples for each test.

iii.3. Pore Size Determination

The light microscope (Zeiss Axiotech 100 HD/DIC) was used to visualize the pores of the scaffolds and control their quality, being the theoretic value of the cubic pores 1000 μm per side. Optical microscopy images were obtained using the ZenCore software and, afterwards, through ImageJ software, the size of each pore (vertical and horizontal central lines) was measured. For each scaffold, the measurements were performed in five faces, including the four lateral faces and top face.

iii.4. Compression Tests

To characterize the mechanical behavior of the 3D scaffolds, compression tests were performed using a custom-made machine, composed by a load cell of 10 N, an actuator with a load capacity of 12 kg and a resolution of 3.05×10^{-4} mm and a flat-ended cylindrical indenter with a diameter of 20 mm (Figure 1). The scaffolds were firstly swollen in ddH_2O for 24h at 37 ºC and their dimensions (width×width×height) were obtained using a caliper. Then, a preload of 0.02 N was applied and the samples were loaded at a constant velocity of 10 mm/min. For each concentration, a minimum of three samples were used. The tests were performed under two different conditions: (I) at room temperature, and (II) at 37 ºC using a saline bath.

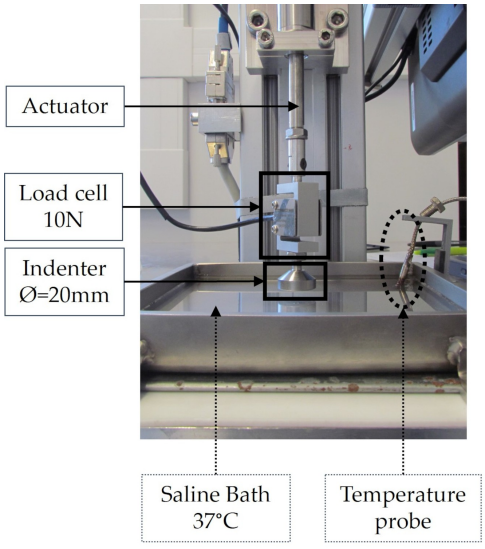

Figure 1: Mechanical set-up used to perform the mechanical tests. The different components are represented, including the actuator, load cell and indenter, which are common to the two testing conditions. The temperature probe and the saline bath were only used when the test was performed at 37 ºC (figure by authors).

Compression data analysis The force-displacement data was acquired directly from the machine software at a rate sampling of 100 Hz. Due to fluctuations in the sampling, interpolation was applied to regularize the data of individual samples. In this way, the statistical treatment could be carried out properly considering the following:

1. it considers each experimental curve, c_j^i

$$i \in \{1, ..., n\} : i, n \in N$$

of the form

$$c_j^i = (f_j, d_j)$$

with a total of j

$$j \in \{1, ..., m\} : j, m \in N$$

experimental data points, as an individual experiment

2. it considers that all the curves c^i describe the same phenomenon, i.e. the same testing protocol is applied to (n) identical samples corresponding to the same agarose:GelMA ratio

After regularization via interpolation, it is possible to apply a point-wise statistical treatment to the curves of a given concentration, calculating:

(a) a mean curve c^{mean} representative of each concentration

(b) statistical quantities such as the standard deviation and the standard error of the mean

Through the mean curve c^{mean}, force-displacement (f, d) can be converted to stress-strain (σ, ϵ), given that all samples have the same geometry and material. Assuming the stress-strain curve, the Young's modulus (E_{mean}) was calculated (Equation 3) considering the slope of the first linear region.

$$E = \frac{\sigma}{\epsilon} \tag{3}$$

Moreover, with the standard deviation of the c^{mean}, the curves corresponding to the upper and bottom limits were obtained, i.e. $c^{mean+std}$ and $c^{mean-std}$. Then, for each of these curves, the Young's modulus was calculated as well: $E_{mean+std}$ and $E_{mean-std}$, respectively. With these values, the deviation associated to E_{mean} was calculated as the difference between them and E_{mean}. In figure below (Figure 2), an example is presented.

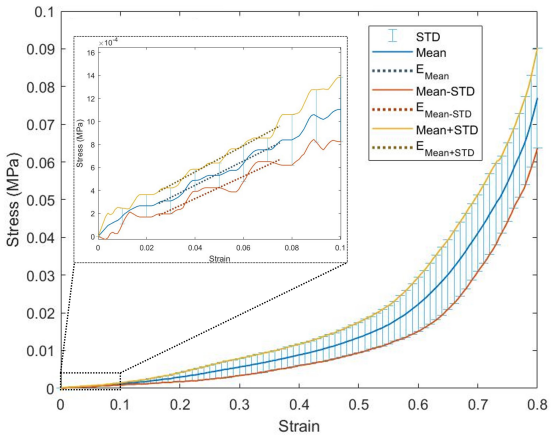

Figure 2: An example of a mean stress-strain curve with the standard deviation and the corresponding curves at the bottom and upper deviations (full lines). A zoom in of the region of interest is presented in the dashed box and it has represented the slope (i.e. Young's modulus, E) of each curve in the first linear region, 2.5-7.5% (dashed lines) (figure by authors).

iii.5. Rheology Analysis

Viscometry tests were performed on the solution of each concentration. 300 μl of solution was poured in the bottom plate and the top spindle, with a diameter of 25 mm, was lowered until reach a gap of 0.3 mm. The viscosity, in mPa.s, was recorded in a total of 30 points for a shear rate from 0.1 to 1000 s^{-1}.

In addition, rheology tests were carried out using swollen discs (diameter = 14 mm and heigh = 1 mm), which were placed in ddH_2O at 37ºC for

24h, to investigate the viscoelastic properties of the material. The top spindle had a diameter of 15 mm and it was lowered until a force between 0.6 N and 1 N was reached. The loss modulus (G''), storage modulus (G') and complex shear modulus (G*) were obtained for 50 points using a strain of 0.1% with an oscillation frequency ranging from 0.1 Hz to 10 Hz. Both analysis were performed using a rheometer Physica MCR-301 (Anton Paar, Sint-Martens-Latem, Belgium), at 37 ºC, with a minimum of 3 samples.

iv. Cell Culture Experiments

The scaffolds were sterilized using ethanol (EtOH) 70% for a minimum of 24h, for which the EtOH solution was refreshed after 12h. Prior to seeding, scaffolds were washed with phosphate-buffered solution (PBS) for a minimum of 1h to remove all the residues of EtOH. For each time point, 3 scaffolds with dimensions of $5\times5\times5$ mm^3 were used and placed in a non-treated 48-well plate, for further sterilization using UV-C irradiation for 30 minutes. After that time, the cells were seeded at a density of 50 000 cells per scaffold (30 μl of cells solution) and the scaffolds were incubated at 37 ºC for 1h to ensure cell adhesion. 500-550 μl of culture medium (DMEM supplemented with 10% FBS and 1% penicillin/streptomycin) was added to each scaffold and incubated again at 37 ºC. The culture medium was refreshed every 2-3 days. For this study, ADSCs in passage 7 were used.

iv.1. MTS Assay

The cell viability was assessed via MTS assay. To this end, the culture medium of each scaffold was replaced by 400 μl of fresh medium with 40 μl of MTS staining, being in the dark for 1.5h to let the solution react. Afterwards, 100 μl of each sample was pipetted into a 96-well plate, twice. The absorbance at 490 nm and 750 nm was assessed using the Infinite 200 PRO microplate reader from Tecan (Mannedorf, Switzerland).

iv.2. Live/Dead Assay

Cell viability was also assessed through a live/dead viability assay using calcein-acetoxymethyl (Ca-AM) and propidium iodide (PI). The staining solution consisted of 8 ml of PBS, 16 μl of Ca-MA and 16 μl of PI (i.e. for every 1 ml of PBS, 2 μl of each stain are added). About 650 μl of the final solution was added to each scaffold and incubated in the dark at room temperature for 30 minutes. After that time, the confocal microscope LSM 710 T-PMT from Zeiss (Jena, Germany) was used to visualize the living and the dead cells.

v. Statistical Analysis

All the results correspond to the mean value and standard deviation (mean$\pm$std). The statistical analysis was performed using the independent-samples t-test with p-value$\leq$0.05, using SPSS Statistics software (IBM).

III. Results

Physical, chemical and biological properties were studied using scaffolds and discs, produced with different weight percentage ratios of agarose to GelMA. For all the characterization tests, the influence of the polymers' concentration was assessed. In addition, for the mass swelling ratio and gel fraction, differences between 2D and 3D structures were also evaluated.

i. Physicochemical Characterization

i.1. Mass Swelling Ratio and Gel Fraction

In figures 3 and 4, examples of discs and scaffolds (dry and swollen) are represented.

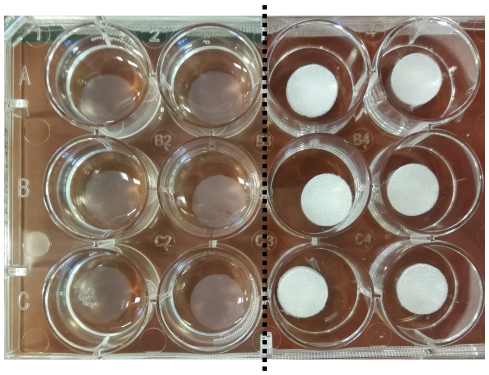

Figure 3: Example of discs used for swelling and gel fraction. On the left, the discs are swollen in ddH_2O at 37 ºC and on the right they are dried (figure by authors).

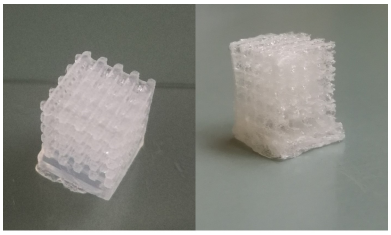

(A) (B)

Figure 4: Example of a scaffold used for swelling and gel fraction: (A) swollen scaffold, and (B) dried scaffold (figure by authors).

The results of mass swelling ratio and gel fraction are presented in figure 5.

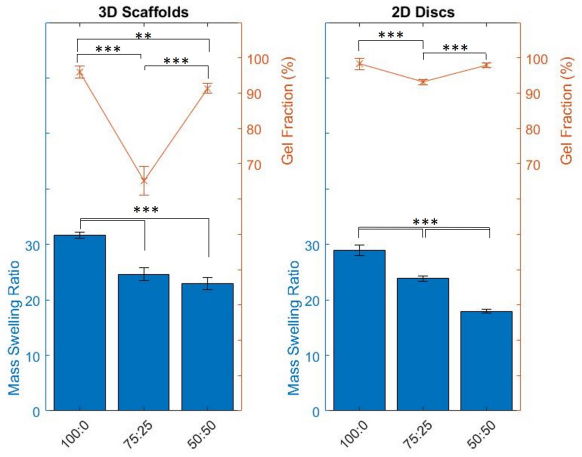

Figure 5: Mass swelling ratio and gel fraction results for 3D scaffolds (left graph) and for 2D discs (right graph). *** p-value$\leq$0.001; ** p-value$\leq$0.01 (figure by authors).

For both 2D and 3D structures, the mass swelling ratio decreases as the concentration of GelMA increases, while for the gel fraction, this trend is not observed, with the lowest values found for the scaffolds and discs of ratio 75:25.

The results for the 3D scaffolds show that, concerning the mass swelling ratio, the two solutions with GelMA (ratios 75:25 and 50:50) were statistically different from the scaffolds with only agarose (ratio 100:0), with p-value$\leq$0.001. On the other hand, gel fractions for each concentration are statistically different, with a p-value$\leq$0.001 between 100:0 and 50:50 ratios and a p-value$\leq$0.01 between 100:0 and 50:50 ratios. In terms of statistical analysis for the discs, the mass swelling ratio was statistically different for all the concentrations, with p-value$\leq$0.001. On the other hand, the gel fraction was only statistically different for the ratio 75:25, when comparing with the other ratios tested (p-value$\leq$0.001). The numerical results are presented in table I.

i.2. Pore Size

In figure 6, a side view and a top view are presented, from a scaffold with ratio of 75:25.

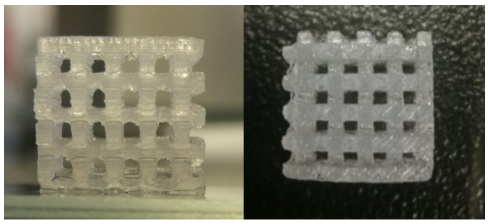

(A) (B)

Figure 6: Example of a scaffold with ratio 75:25: (A) side-view, and (B) top-view (figure by authors).

The light microscope was used to assess the quality of those scaffolds. A side view and a top view of one single pore are presented in figure 7.

Table I: Results for the mass swelling ratio and gel fraction for the ratios 100:0, 75:25 and 50:50 (agarose:GelMA), considering scaffolds and discs (table by authors).

	3D Scaffolds		2D Discs	
Ratios	**Mass Swelling Ratio**	**Gel Fraction (%)**	**Mass Swelling Ratio**	**Gel Fraction (%)**
100:0	31.61±0.55	95.93±1.72	28.97±0.97	98.27±1.56
75:25	24.64±1.21	65.07±4.06	23.88±0.49	93.17±0.75
50:50	22.98±1.12	91.36±1.47	17.96±0.35	97.85±0.60

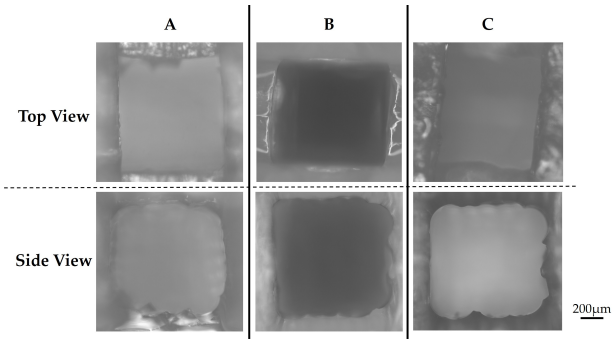

Figure 7: Light microscopy images for agarose and GelMA in ratios (A) 100:0, (B) 75:25 and (C) 50:50. Top row images correspond to the top face of the scaffolds and the bottom row images correspond to the side face of the scaffolds (figure by authors).

The pore size result for the ratio 100:0 is 0.999±0.082 mm, for the ratio 75:25 is 1.004±0.082 mm and for the ratio 50:50 is 1.037±0.077 mm. The theoretical value for each pore is 1000 μm each side, which indicates an excellent CAD/CAM mimicry

i.3. Compression Tests

Compression tests were performed to assess the mechanical behavior of the 3D scaffolds. To complement the design of this experiment, scaffolds of 100% w/v GelMA (i.e. ratio 0:100) were also considered, since to date, mechanical tests of GelMA scaffolds were not performed under the same testing conditions of this study. The experimental tests were performed using a minimum of three samples per testing condition.

Figure 8 shows all the stress-strain mean curves obtained for all concentrations at two different testing conditions: at room temperature and at physiological temperature, which corresponds to 37 ºC.

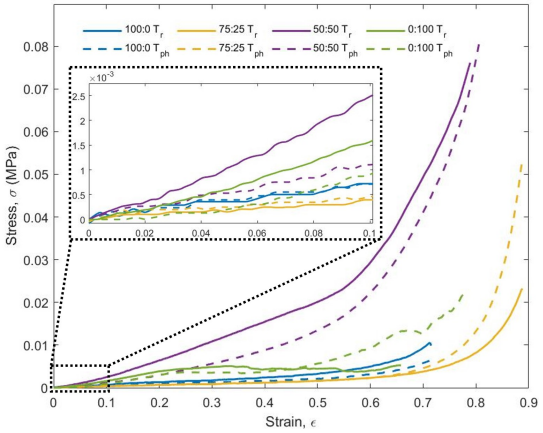

Figure 8: Stress-strain mean curves obtained for the different ratios analyzed: 100:0, 75:25, 50:50, 0:100 (agarose:GelMA) at two different testing conditions: at room temperature (T_r - full lines) and at 37ºC using a saline bath (physiological temperature T_{ph} - dashed lines). The dotted region represents the curves until 10% strain (figure by authors).

The Young's modulus was calculated through the slope of the first linear region of the loading curve, assuming a strain range between 2.5% and 7.5% (Delaine-Smith et al. 2016).

In table II, the results obtained are presented, along with the corresponding deviations.

Table II: Young's modulus ± deviation results for the different ratios analyzed: 100:0, 75:25, 50:50, 0:100 (agarose:GelMA) at room temperature (T_r), and at physiological temperature (T_{ph}) (table by authors).

		Young's Modulus (kPa)
100:0	T_r	4.93
	T_{ph}	7.13
75:25	T_r	2.86
	T_{ph}	3.47
50:50	T_r	25.11
	T_{ph}	10.55
0:100	T_r	16.41
	T_{ph}	8.44

From the results, different behaviors are observed for the different ratios considered. When agarose is the main component, such as the ratios of 100:0 and 75:25, the increase of temperature and the presence of a saline bath, increases the stiffness of the scaffold. However, when the percentage of GelMA increases, such as for the ratios of 50:50 and 0:100, the inverse behavior is observed. Increasing the temperature, using a saline bath, makes the scaffold softer (decreased stiffness).

Comparing all the scaffolds tested, either at 37 ºC or at room temperature, the scaffolds of ratio 50:50 are the stiffest, while the softest are those of ratio 75:25.

i.4. Rheology Analysis

First, a viscosity measurement was performed, being the result represented in the following graph (Figure 9).

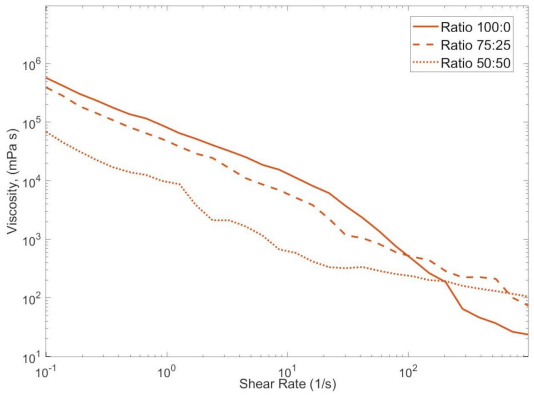

Figure 9: Viscosity results (mPa.s) in logarithmic scale. Full line corresponds to ratio 100:0; Dashed line corresponds to ratio 75:25; Dotted line corresponds to ratio 50:50 (figure by authors).

The curves obtained show that viscosity of agarose:GelMA blends is lower than agarose only blends, which indicates that GelMA makes the hydrogel less viscous, becoming a more fluid solution.

Figure 10 represents the results of rheology, such as the complex shear modulus (G*), the storage modulus (G') and the loss modulus (G''), for each ratio of agarose:GelMA studied.

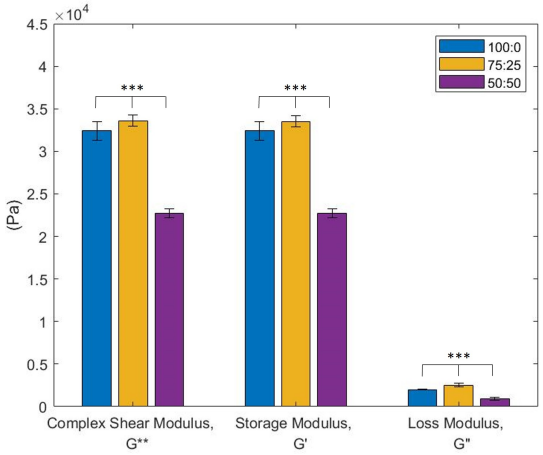

Figure 10: Rheology results: complex shear modulus (G*), storage modulus (G') and loss modulus (G''), for the ratios of 100:0, 75:25 and 50:50 (agarose:GelMA). *** p-value≤0.001 (figure by authors).

The numeric values are represented in table III.

The modulus for the ratio of 75:25 was the highest, while the ratio 50:50 evidenced the lowest re-

Table III: Numeric results (mean±std) of the complex shear modulus, storage modulus, loss modulus and loss tangent for the ratios 100:0, 75:25 and 50:50 (agarose:GelMA) (table by authors).

Ratios	Complex Shear Modulus G* (Pa)	Storage Modulus G′ (Pa)	Loss Modulus G″ (Pa)	Loss Tangent $tan\delta$
100:0	$3.50x10^4 \pm 1.12x10^3$	$3.49x10^4 \pm 1.13x10^3$	$2.11x10^3 \pm 5.29x10^1$	0.062 ± 0.002
75:25	$3.26x10^4 \pm 2.61x10^2$	$3.26x10^4 \pm 2.74x10^2$	$2.33x10^3 \pm 1.77x10^2$	0.075 ± 0.008
50:50	$2.27x10^4 \pm 5.06x10^2$	$2.27x10^4 \pm 5.13x10^2$	$9.13x10^2 \pm 1.62x10^2$	0.040 ± 0.008

sults. The statistical analysis shows that different agarose:GelMA ratios display statistically different moduli, with p-value$\leq$0.001.

The loss tangent is the ratio of the loss modulus and the storage modulus. It indicates how elastic ($tan\delta < 1$) or plastic ($tan\delta > 1$) is the material. The corresponding results are presented in table III and they show that all samples exhibit a predominantly elastic behavior ($tan\delta < 1$).

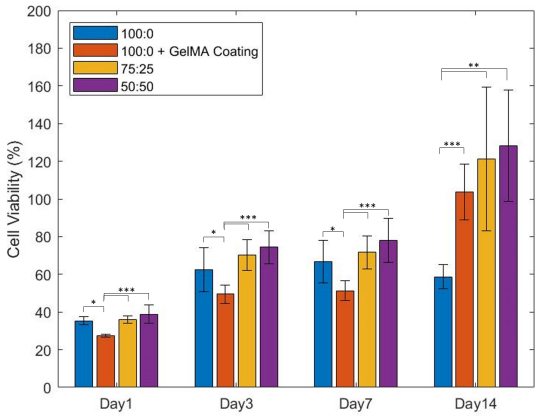

Figure 11: MTS assay results for the different ratios analyzed: 100:0 (1st bar), 100:0 with GelMA coating (2nd bar), 75:25 (3rd bar) and 50:50 (4th bar). *p-value$\leq$0.05, **p-value$\leq$0.01, ***p-value$\leq$0.001 (figure by authors).

ii. Cell Culture Experiments

In addition to the concentrations previously presented, we also assessed if a GelMA coating on the agarose scaffolds (ratio 100:0) would be enough to improve the cell adhesion capacity.

ii.1. MTS Assay

To assess the metabolic activity, an MTS assay was carried out and figure 11 shows the obtained results, which are normalized to tissue culture plastic (TCP) as a positive control.

Table IV presents the numeric values also normalized to TCP.

Taking into account these results, the metabolic activity increases over time, being higher for the scaffolds containing GelMA. For these scaffolds at day 14, the value exceeds the TCP control (i.e. higher than 100%). Moreover, increasing the concentration of GelMA, the metabolic activity increases as well.

According to statistics, at all time points the metabolic activity is statistically different between the scaffolds containing 3% w/v agarose (100:0) and the scaffolds of agarose with GelMA coating (p-value$\leq$0.05 for the first three days and p-value$\leq$0.001 for the last day). For day 1, day 3 and day 7, the results were statistically different between the scaffold with the coating and the two blends with GelMA (p-value$\leq$0.001). At day

Table IV: Cell's viability (%) for each time point, via MTS assay. Results in the format mean±standard deviation (table by authors).

Ratios	Day 1	Day 3	Day 7	Day 14
100:0	35.37±2.01	62.38±11.65	66.66±11.26	58.67±6.38
100:0 + GelMA Coating	27.47±0.80	49.42±4.86	51.30+±5.22	103.80±14.80
75:25	35.98±1.81	70.15±8.07	71.61±8.86	121.30±38.17
50:50	38.88±4.95	74.43±8.81	77.99±11.52	128.30±29.55

14, it was also significantly different between the ratio 100:0 and the two ratios with GelMA (p-value$\leq$0.01).

Moreover, to complement the MTS results, confocal microscope images were obtained.

ii.2. Live/Dead Assay

The confocal images are represented in figure 12.

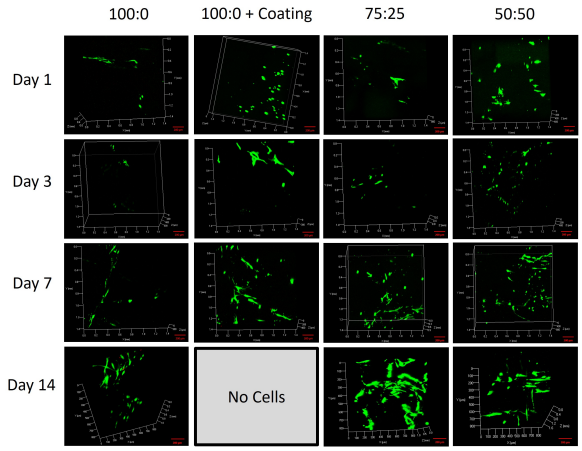

Figure 12: 3D confocal microscope images of an area of interest of the scaffolds for each time point of the experiment (rows). Each column corresponds to a different scaffold in the following order from left to right: 100:0, 100:0 with GelMA coating, ratio 75:25, and ratio 50:50. Scale bars of 200 μm (red lines at the bottom right of each image) (figure by authors).

In contrast to the MTS assay, there were no visible cells attached to the scaffolds of agarose with coating on day 14. This might indicate the presence of stem cells in the well instead of on the scaffolds.

For all the concentrations, there is a decrease in cell density on day 3, however, it tends to increase on days 7 and 14.

Even though, the metabolic activity for the 100:0 scaffold decreases on day 14 as shown in the MTS assay, the confocal images showed a higher density of cells, however, the cells tend to have a spherical morphology. Furthermore, a higher quantity of dead cells are present on day 14, resulting in a reduction of the viability correlated to the live/dead imaging.

The most promising results are obtained for the scaffolds consisting of both GelMA and agarose, which is in accordance with the MTS assay. In the scaffolds with GelMA, the cells tend to stretch and spread over the hydrogel area. It was observed that in the scaffold with higher concentration of GelMA, cells tend to stretch and spread earlier. However, at the day 14, the cells have similar morphology for both concentrations of GelMA used in this study

IV. Discussion

Tissue engineering is a promising approach to regenerate and repair damaged tissues. The development of patient-specific solutions, which mimic the native tissue of the patient, are the future of clinical treatments, with potential for replacing current approaches such as prosthesis and implants. This next generation of solutions is based on the combination of biomaterials with cells, creating a scaffold able to regenerate a specific tissue.

In this study, scaffolds were produced via indirect 3D printing, specifically for adipose tissue regeneration purposes. By combining agarose and GelMA with ADSCs, good outcomes were

achieved. The structures were characterized in terms of physico-chemical properties, and then biological assessments were performed.

In terms of pore size measurements, an excellent result was obtained when comparing the experimental pore size with the theoretical value, validating the quality of the experimental protocol.

The capacity to uptake water is an important feature for the hydrogel to ensure the cell's viability in cell culture experiments (Zarrintaj et al. 2018), since a higher mass swelling ratio increases the diffusion of nutrients and waste products (Van Hoorick et al. 2015). For both scaffolds and discs produced in this study, the mass swelling ratio significantly decreased with the increase of GelMA, which was also concluded by Dravid et al. (2022), who used agarose with gelatin type A. On the other hand, increasing the GelMA concentration, there was no clear trend on the gel fraction. A comparison with results from scaffolds consisting of 10% w/v GelMA reported in (Van Damme et al. 2020), allowed us to conclude that the addition of agarose, resulted in an increase of both gel fraction and mass swelling ratio. Van Damme et al. (2020) obtained a gel fraction of 66.11$\pm$1.13% and a mass swelling ratio around 16 for 3D scaffolds produced via indirect printing. Considering the mass swelling ratio of 100:0, which means the scaffold is composed only of agarose, our results are in accordance with the work of Su et al. (2021), which obtained a value of 30.7.

In terms of compression modulus, the crosslinking, the increase in temperature and the saline bath influence the results significantly. Comparing the stiffness of all scaffolds, the ratio 75:25 produced the softest scaffolds, which might be due to the leaching of the 25% of GelMA molecules, leading to a structure that is not fully crosslinked, as it is reflected in the gel fraction. This ratio might have impaired the crosslinking capability of the GelMA, due to the distance between the functional groups and the steric hindrance of the agarose. Therefore, when comparing with 100:0 scaffolds (agarose only), the stiffness decreases. On the other hand, the ratio 50:50 created the stiffest scaffolds. A possible explanation for this observation might be when these two hydrogels are combined at an equal amount, the hydroxyl groups (-OH) of agarose and the carbonyl groups (C=O) of gelatin would interact, creating a synergistic physical effect, enhancing the mechanical strength of the scaffold. Increasing the GelMA up to 50% w/v, allows the creation of new connections, such as ionic electrostatic bonds (Imani et al. 2012), which are stronger than hydrogen bonds. Whereas, for the scaffolds of only GelMA (0:100), hydrogen bonds will prevail again and therefore the stiffness decreases.

The same observation was pointed out by Imani et al. (2012) in which the ratio of 50:50 of agarose and gelatin type-A was the ideal solution in terms of integral stability, attributing that observation to the more electrostatic interactions between the agarose and gelatin chains.

Moreover, the effect of the physiological conditions differed in the different ratios used. When agarose was the predominant hydrogel, the saline bath and the temperature caused an increase in the stiffness of the structure. These conditions might have created a more incompressible material as well as cause some expulsion of water from the scaffolds. On the other hand, when there is a higher amount of GelMA (i.e. 50:50 and 0:100 ratios), the physiological conditions might have increased the flexibility of the GelMA chains, which in turn increased the water uptake, resulting in a softer structure when compared to the dry and room temperature conditions.

Comparing with the result of Van Damme et al. (2020), the scaffold composed solely by GelMA has a very different Young's modulus value. That difference might be related to the different test parameters, such as preload, which has been in-

vestigated to have influence on the mechanical behavior (Teixeira 2018, Krouskop et al. 1998). In literature, Sakai et al. (2007) and Dravid et al. (2022) studied the mechanical properties of blends of agarose with gelatin. The stress-strain curves of the present work are comparable with the ones reported in literature, showing that the mechanical behavior is similar to the other blends. However, further comparison is not reliable since Sakai et al. (2007) and Dravid et al. (2022) used different variations of the materials, including the agarose, gelatin and solvent, as well as different testing parameters.

Regarding the characterization of agarose as such, it is more common to find studies with samples in a cylindrical shape, formed by a homogeneous solution. For Su et al. (2021) a 2% agarose gel had an elastic modulus of 196 kPa while Buckley et al. (2009) measured a ramp modulus of 55.6$\pm$0.5kPa. Both studies reported a modulus higher than the results of the present study, which might be explained by the samples' geometry and testing parameters. Buckley et al. (2009) also observed that increasing the agarose concentration, the modulus increased and that testing the gels at 37ºC, the modulus decreased. The authors associate the temperature dependent properties to the dissociation of helix bundles and melting of helices, however they used an agarose with a low gelling point, which is different from the present study.

Concerning tissue engineering, in literature, the Young's modulus of human adipose breast tissue has a wide variety of values. This phenomenon is related to the different testing parameters used to evaluate the mechanical properties (Teixeira & Martins 2023). Elastic modulus results from 0.7$\pm$0.2 kPa (Matsumura et al. 2009) to 24$\pm$6 kPa (Krouskop et al. 1998) can be found in literature for *ex-vivo* experiments, while for *in-vivo* experiments the elastic modulus vary between 0.33 kPa (Chen et al. 2013) to 23.54$\pm$4.03 kPa (Van Houten et al. 2003). Due to this variety found in the mechanical properties of adipose tissue, the results of the present study are in accordance with the literature. Therefore, in terms of mechanical stability, the scaffolds proposed in this study are possible solutions to support adipose tissue regeneration due to their mechanocompatibility.

Looking into the rheology properties, the viscosity results show that increasing the GelMA content, the solution becomes more fluid at 37 ºC. Increasing the shear rates, the viscosity decreases for all the blends, exhibiting shear-thinning behavior, which is a feature of non-Newtonian materials, such as agarose and gelatin. These results are in accordance with the studies of Imani et al. (2012), Dravid et al. (2022) and Fernández et al. (2007).

For the storage modulus (G'), loss modulus (G'') and complex shear modulus (G*), generally all decreased with the addition of gelatin for the ratio of 50:50. Awad et al. (2004) also concluded that the complex shear modulus of agarose is higher than the one of gelatin. Since the storage modulus was higher than the loss modulus (G'> G''), the blend presented a more elastic behavior. Adding GelMA, the loss tangent decreased for the ratio of 50:50, which was also concluded by Dravid et al. (2022). Additionally, for Awad et al. (2004), the phase angle (δ) for agarose and gelatin was less than 15º, which indicates that both hydrogels behave like viscoelastic solids. Only studying agarose, Barrangou et al. (2006) also reported low phase angles and that the storage moduli values depended on frequency, which is a typical feature of a viscoelastic gel.

When looking at all the physico-chemical properties, an evident correlation can be pointed out between gel fraction, compression and rheology. The concentration of 75:25 presents the lowest gel fraction value and the lowest stiffness, which indicates that the low degree of crosslinks has an impact on the mechanical stability of the scaffolds at quasi-static loads. On the other hand, using dy-

namic loads, the 75:25 scaffolds have the highest storage (G') and loss (G'') moduli.

Regarding the *in-vitro* culture experiments, using ADSCs, the metabolic activity increased over the time of the experiment for the blends with GelMA, while for the scaffold with only agarose, it increased until day 7 but decreased on day 14. The cells' morphology in the scaffolds of only agarose tend to have a spherical shape due to the lack of extracellular motives for cells to attach, indicating that pure agarose does not promote cell adhesion and proliferation. With ADSCs in agarose scaffolds, Awad et al. (2004) observed the same cell morphology, with a cell viability higher than 95%. Even though Imani et al. (2012) used different cells (i.e. hamster ovary cells), they also noted that the cells in scaffolds of agarose tended to form aggregates, due to the lack of cell moieties, with a cell viability near 100%. The same observation was reported by Su et al. (2021) with agarose scaffolds, where cells (MRC-5 and RS1) tended to have a spherical shape with cell viability around 80%.

Applying a coating of GelMA in agarose scaffolds also did not work effectively, since the coating tended to detach from the scaffold. This might have happened since the scaffolds were sterilized in EtOH 70% prior to cell culture, which left the scaffolds in a semi-dehydrated state. Then, the scaffolds were placed in PBS to hydrate and swell, increasing their volume, which might have induced stress within the hydrogel and, hence, leading to coating detachment (Prucker et al. 2018). As the coating will most likely still be present in the well plate while performing the MTS assay, a positive MTS result could be observed for the day 14 samples, whereas no cells could be observed on the scaffolds following the live/dead staining. Even though this approach was not successful, there is margin for improvement and the technique can be optimized by testing different immersion times and/or coating thicknesses (i.e. multiple layers of coating might improve adhesion). In addition, a different coating method, such as spray coating, can be tested as well as a surface modification or chemical functionalization can be applied to the agarose scaffold surface, prior coating, to increase the adhesion with GelMA.

On the other hand, when the GelMA is mixed with agarose, the results are promising. The metabolic activity was higher than control (>100%) at day 14, with cells in a high density presenting their typical stretched morphology. Therefore, the results prove the good biocompatibility (i.e. low cytotoxicity) of the scaffolds of agarose and GelMA at the ratios 75:25 and 50:50. Imani et al. (2012) obtained the highest cell viability (using hamster ovary cells) for the scaffolds with ratio 50:50 (agarose:gelatin), being 20% above control, however, they did not observe significant cell spreading when compared with control. On the other hand, Sakai et al. (2007) seeded CRFK cells into agarose-gelatin hydrogels, with cells starting to spread after 4h of culture and reaching a cell viability around 80%. Using the same hydrogelsbut seeded with SH-SY5Y cells, Dravid et al. (2022) obtained a cell viability around 90%. Considering gelatin scaffolds, Awad et al. (2004) showed that ADSCs exhibited a polygonal shape with a cell viability higher than 95%. Van Damme et al. (2021) obtained a cell viability higher than 85%, but did not obtained a stretch morphology for ADSCs seeded in films of GelMA with high degree of substitution. Moreover, looking to the study of Tytgat et al. (2019), the results of the MTS assay show a proliferation rate between day 1 and day 7 of 155% and between day 7 and day 14 of 118%, which is comparable with the results of the present study. The blend of agarose with GelMA presents high cell metabolic activity, i.e. cell viability, and, hence, cell proliferation.

V. Conclusion

Adipose tissue regeneration is a promising alternative for the current clinical approaches in breast reconstruction, such as silicone implants or fat grafting. Even though advancements have been made in research to present a solution, more studies need to be carried out to find the ideal scaffold. In this work it was presented a new combination of biomaterials for this purpose. Scaffolds developed using a blend of agarose and GelMA were successfully produced and characterized, overcoming the limitations of each one when used individually. This blend showed good outcomes, especially in terms of mechanical stability and cell adhesion. The optimum composition, regarding cells' viability, is the ratio of 50:50, nevertheless, the ratio of 75:25 also presents good outcomes in terms of cell's viability, forming softer structures. For future work, more *in-vitro* characterization and *in-vivo* experiments should be implemented to assess the scaffold potential for tissue regeneration.

References

Aliabouzar, M., Zhang, G. L. & Sarkar, K. (2018), 'Acoustic and mechanical characterization of 3D-printed scaffolds for tissue engineering applications', *Biomedical Materials (Bristol)* **13**(5). DOI: 10.1088/1748-605X/aad417.

Awad, H. A., Wickham, M. Q., Leddy, H. A., Gimble, J. M. & Guilak, F. (2004), 'Chondrogenic differentiation of adipose-derived adult stem cells in agarose, alginate, and gelatin scaffolds', *Biomaterials* **25**, 3211–3222. DOI: 10.1016/j.biomaterials.2003.10.045.

Barrangou, L. M., Daubert, C. R. & Foegeding, E. A. (2006), 'Textural properties of agarose gels. i. rheological and fracture properties', *Food Hydrocolloids* **20**, 184–195. DOI: 10.1016/j.foodhyd.2005.02.019.

Bramhe, P., Rarokar, N., Kumbhalkar, R., Saoji, S. & Khedekar, P. (2024), 'Natural and synthetic polymeric hydrogel: A bioink for 3d bioprinting of tissue models', *Journal of Drug Delivery Science and Technology* **101**.

Buckley, C. T., Thorpe, S. D., O'Brien, F. J., Robinson, A. J. & Kelly, D. J. (2009), 'The effect of concentration, thermal history and cell seeding density on the initial mechanical properties of agarose hydrogels', *Journal of the Mechanical Behavior of Biomedical Materials* **2**, 512–521. DOI: 10.1016/j.jmbbm.2008.12.007.

Bulcke, A. I. V. D., Bogdanov, B., Rooze, N. D., Schacht, E. H., Cornelissen, M. & Berghmans, H. (2000), 'Structural and rheological properties of methacrylamide modified gelatin hydrogels', *Biomacromolecules* **1**, 31–38. DOI: 10.1021/bm990017d.

Bülow, A., Schäfer, B. & Beier, J. P. (2023), 'Three-dimensional bioprinting in soft tissue engineering for plastic and reconstructive surgery', *Bioengineering* **10**.

Chen, J., Brandt, K., Ghosh, K., Grimm, R., Glaser, K., Kugel, J. & Ehman, R. (2013), 'Noncompressive MR Elastography of Breasts', *Proc. Intl. Soc. Mag. Reson. Med.* **21**(6), 1736.

Cleversey, C., Robinson, M. & Willerth, S. M. (2019), '3D printing breast tissue models: A review of past work and directions for future work', *Micromachines* **10**(8). DOI: 10.3390/mi10080501.

Delaine-Smith, R. M., Burney, S., Balkwill, F. R. & Knight, M. M. (2016), 'Experimental validation of a flat punch indentation methodology calibrated against unconfined compression tests for determination of soft tissue biomechanics', *Journal of the Mechanical Behavior of Biomedical Materials* **60**, 401–415. DOI: 10.1016/j.jmbbm.2016.02.019.

Donate, R., Alemán-Domínguez, M. E. & Monzón, M. (2021), 'On the effectiveness of oxygen plasma and alkali surface treatments to modify the properties of polylactic acid scaffolds', *Polymers* **13**. DOI: 10.3390/polym13101643.

Donnely, E., Griffin, M. & Butler, P. E. (2020), 'Breast Reconstruction with a Tissue Engineering and Regenerative Medicine Approach (Systematic Review)', *Annals of Biomedical Engineering* **48**(1), 9–25. DOI: 10.1007/s10439-019-02373-3.

Dravid, A., McCaughey-Chapman, A., Raos, B., O'Carroll, S. J., Connor, B. & Svirskis, D. (2022), 'Development of agarose–gelatin bioinks for extrusion-based bioprinting and cell encapsulation', *Biomedical Materials* **17**, 055001. DOI: 10.1088/1748-605X/ac759f.

Fernández, E., López, D., Mijangos, C., Duskova-Smrckova, M., Ilavsky, M. & Dusek, K. (2007), 'Rheological and thermal properties of agarose aqueous solutions and hydrogels', *Journal of Polymer Science: Part B: Polymer Physics* **46**, 322–328. DOI: 10.1002/polb.21370.

Imani, R., Emami, S. H., Moshtagh, P. R., Baheiraei, N. & Sharifi, A. M. (2012), 'Preparation and characterization of agarose-gelatin blend hydrogels as a cell encapsulation matrix: An in-vitro study', *Journal of Macromolecular Science, Part B: Physics* **51**, 1606–1616. DOI: 10.1080/00222348.2012.657110.

Jiang, F., Xu, X. W., Chen, F. Q., Weng, H. F., Chen, J., Ru, Y., Xiao, Q. & Xiao, A. F. (2023), 'Extraction, modification and biomedical application of agarose hydrogels: A review', *Marine Drugs* **21**.

Krouskop, T. A., Wheeler, T. M., Kallel, F., Garra, B. S. & Hall, T. (1998), 'Elastic Moduli of Breast and Prostate Tissues under Compression', *Ultrasonic Imaging* **20**(4), 260–274. DOI: 10.1177/016173469802000403.

Li, X., Ding, W., Wang, S., Yang, L., Yu, Q., Xiao, C., Chen, G., Zhang, L., Guan, S. & Sun, D. (2023), 'Three-dimensional sulfated bacterial cellulose/gelatin composite scaffolds for culturing hepatocytes', *Cyborg and Bionic Systems* **4**.

Markovic, M., Hölzl, J. V. H. K., Tromayer, M., Gruber, P., Nürnberger, S., Dubruel, P., Vlierberghe, S. V., Liska, R. & Ovsianikov, A. (2015), 'Hybrid Tissue Engineering Scaffolds by Combination of Three-Dimensional Printing and Cell Photoencapsulation', *Journal of Nanotechnology in Engineering and Medicine* **6**(2), 7. DOI: 10.1115/1.4031466.

Matsumura, T., Umemoto, T., Fujihara, Y., Ueno, E., Yamakawa, M., Shiina, T. & Mitake, T. (2009), 'Measurement of elastic property of breast tissue for elasticity imaging', *Proceedings - IEEE Ultrasonics Symposium* pp. 1451–1454. DOI: 10.1109/ULTSYM.2009.5442044.

O'Halloran, N., Potter, S., Kerin, M. & Lowery, A. (2018), 'Recent Advances and Future Directions in Postmastectomy Breast Reconstruction', *Clinical Breast Cancer* **18**(4), e571–e585. DOI: 10.1016/j.clbc.2018.02.004.

Ovsianikov, A., Deiwick, A., Van Vlierberghe, S., Pflaum, M., Wilhelmi, M., Dubruel, P. & Chichkov, B. (2010), 'Laser fabrication of 3D gelatin scaffolds for the generation of bioartificial tissues', *Materials* **4**(1), 288–299. DOI: 10.3390/ma4010288.

Peirsman, A., Nguyen, H. T., Waeyenberge, M. V., Ceballos, C., Bolivar, J., Kawakita, S., Vanlauwe, F., Tirpáková, Z., Dorpe, S. V., Damme, L. V., Mecwan, M., Ermis, M., Maity, S., Mandal, K., Herculano, R., Depypere, B., Budiharto, L., Vlierberghe, S. V., Wever, O. D., Blondeel, P., Jucaud, V., Dokmeci, M. R. & Khademhosseini, A. (2023), 'Vascularized adipose tissue engineering: moving towards soft tissue reconstruction', *Biofabrication* **15**.

Prucker, O., Brandstetter, T. & Rühe, J. (2018), 'Surface-attached hydrogel coatings via c,h-insertion crosslinking for biomedical and bioanalytical applications (review)', *Biointerphases* **13**. DOI: 10.1116/1.4999786.

Sakai, S., Hashimoto, I. & Kawakami, K. (2007), 'Synthesis of an agarose-gelatin conjugate for use as a tissue engineering scaffold', *Journal of Bioscience and Bioengineering* **103**, 22–26. DOI: 10.1263/jbb.103.22.

Su, T., Zhang, M., Zeng, Q., Pan, W., Huang, Y., Qian, Y., Dong, W., Qi, X. & Shen, J. (2021), 'Mussel-inspired agarose hydrogel scaffolds for skin tissue engineering', *Bioactive Materials* **6**, 579–588. DOI: 10.1016/j.bioactmat.2020.09.004.

Teixeira, A. M. (2018), 'Mechanical characterisation of an organic phantom candidate for breast tissue'.
URL: *https://repositorio-aberto.up.pt/handle/10216/113744*

Teixeira, A. M. & Martins, P. (2020), 'Mechanical characterisation of an organic phantom candidate for breast tissue', *Journal of Biomaterials Applications* **34**, 1163–1170. DOI: 10.1177/0885328219895738.

Teixeira, A. M. & Martins, P. (2023), 'A review of bioengineering techniques applied to breast tissue: Mechanical properties, tissue engineering and finite element analysis', *Frontiers in Bioengineering and Biotechnology* **11**. DOI: 10.3389/fbioe.2023.1161815.

Tromayer, M., Dobos, A., Gruber, P., Ajami, A., Dedic, R., Ovsianikov, A. & Liska, R. (2018), 'A biocompatible diazosulfonate initiator for direct encapsulation of human stem cells: Via two-photon polymerization', *Polymer Chemistry* **9**, 3108–3117. DOI: 10.1039/c8py00278a.

Tytgat, L., Van Damme, L., Ortega Arevalo, M. d. P., Declercq, H., Thienpont, H., Otteveare, H., Blondeel, P., Dubruel, P. & Van Vlierberghe, S. (2019), 'Extrusion-based 3D printing of photo-crosslinkable gelatin and κ-carrageenan hydrogel blends for adipose tissue regeneration', *International Journal of Biological Macromolecules* **140**, 929–938. DOI: 10.1016/j.ijbiomac.2019.08.124.

Van Damme, L., Briant, E., Blondeel, P. & Sandra, V. (2020), 'Indirect versus direct 3d printing of hydrogel scaffolds for adipose tissue regeneration', *MRS Advances* **5**, 855–864. DOI: 10.1557/adv.2020.117.

Van Damme, L., Van Hoorick, J., Blondeel, P. & Van Vlierberghe, S. (2021), 'Toward adipose tissue engineering using thiol-norbornene photo-crosslinkable gelatin hydrogels', *Biomacromolecules* **22**, 2408–2418.

Van Hoorick, J., Declercq, H., De Muynck, A., Houben, A., Van Hoorebeke, L., Cornelissen, R., Van Erps, J., Thienpont, H., Dubruel, P. & Van Vlierberghe, S. (2015), 'Indirect additive manufacturing as an elegant tool for the production of self-supporting low density gelatin scaffolds', *Journal of Materials Science: Materials in Medicine* **26**(10). DOI: 10.1007/s10856-015-5566-4.

Van Houten, E. E., Doyley, M. M., Kennedy, F. E., Weaver, J. B. & Paulsen, K. D. (2003), 'Initial in vivo experience with steady-state subzone-based MR elastography of the human breast', *Journal of Magnetic Resonance Imaging* **17**(1), 72–85. DOI: 10.1002/jmri.10232.

Xu, Y., Zhang, F., Zhai, W., Cheng, S., Li, J. & Wang, Y. (2022), 'Unraveling of advances in 3d-printed polymer-based bone scaffolds', *Polymers* **14**.

Zarrintaj, P., Manouchehri, S., Ahmadi, Z., Saeb, M. R., Urbanska, A. M., Kaplan, D. L. & Mozafari, M. (2018), 'Agarose-based biomaterials for tissue engineering', *Carbohydrate Polymers* **187**, 66–84. DOI: 10.1016/j.carbpol.2018.01.060.

Zhou, M., Hou, J., Zhang, G., Luo, C., Zeng, Y., Mou, S., Xiao, P., Zhong, A., Yuan, Q., Yang, J., Wang, Z. & Sun, J. (2020), 'Tuning the mechanics of 3D-printed scaffolds by crystal lattice-like structural design for breast tissue engineering', *Biofabrication* **12**(1). DOI: 10.1088/1758-5090/ab52ea.

Zigon-Branc, S., Markovic, M., Hoorick, J. V., Vlierberghe, S. V., Dubruel, P., Zerobin, E., Baudis, S. & Ovsianikov, A. (2019), 'Impact of hydrogel stiffness on differentiation of human adipose-derived stem cell microspheroids', *Tissue Engineering - Part A* **25**, 1369–1380. DOI: 10.1089/ten.tea.2018.0237.